National Center for Preservation Technology and Training (NCPTT) Grant Number: MT-2210-06-NC-02

Project Title: Mechanical Anchor Strength in Stone Masonry

Organizations:
Vertical Access LLC
The Association for Preservation Technology International (APTI)

Principal Investigator: Kelly Streeter, P.E.

Project Team: Kelly Streeter, Vertical Access LLC
Keith Luscinski, Vertical Access LLC
Kent Diebolt, Vertical Access LLC
Michael Schuller, Atkinson-Noland & Associates Inc.

Contact Information:
Kelly Streeter
Vertical Access LLC
48 Moose Hill Road
Guilford, CT 06437
(917) 749-0998
kelly@vertical-access.com

TABLE OF CONTENTS

TABLE OF FIGURES

TABLE OF TABLES

1. Executive Summary

The main objective of this research project is to better understand the failure strength and the modes of failure of different types of mechanical anchor systems in stone masonry. A secondary objective is to discover whether various non-destructive methods for evaluation of physical properties applied to the stone specimens helps to predict the tension and shear strength of the mechanical anchors.

2. Introduction

Mechanical anchor systems, such as Powers Power-Studs and Powers Wedge-Bolts, are commonly used in historic masonry materials including limestone and sandstone despite the lack of design values for this type of base material. Scaffolding lateral supports, signage installations and telecommunication mounting systems all use these mechanical fasteners in limestone, sandstone and other natural stone materials.

Figure 2.1: Mechanical anchor damage in facade

The current lack of codes, guidelines or recommendations for pull-out and shear values of these anchors in historic masonry materials leaves the design community to improvise the design and specification of these anchors. Guidelines such as "Appendix A, Guidelines for Seismic Retrofit of Existing Buildings" in the 2003 International Existing Building Code [International Code Council 2001], ASTM Standard "E488-96: Standard Test Methods for Strength of Anchors in Concrete and Masonry Elements" [ASTM 2003] and "Acceptance Criteria for Expansion Anchors in Concrete and Masonry Elements" [ICC Evaluation Services 2005] are only relevant to concrete and brick masonry. Although field-testing is employed for some projects, more commonly an arbitrary reduction of the ultimate yield values is used when designing these elements for use in natural stone. The creation of a standard or empirical design equation for these values is arduous because, unlike concrete and concrete masonry units, historic building stone units are not manufactured in a controlled environment, and their physical properties such as density and compressive strength vary from quarry to quarry and within quarry strata.

The primary inspiration for this project is the dearth of applicable field research in mechanical expansion and thread-type anchors in contrast to the many shear and pull-out investigations of injection or adhesive anchors. Research into adhesive anchors has been carried out by the construction industry as well as peripheral fields that have some application to building preservation and the study of masonry, such as geotechnology and civil engineering. In one scientific study intended for application to recreational rock climbing, masonry anchors were installed and tested in a soft South African sandstone. In this study, most of the anchors were adhesive-type anchors, but a mechanical anchor was also evaluated. The pull-out and shear values of the anchors were determined and the mode of failure evaluated [Jarvis and Hyman 2000].

The research that has been published on mechanical anchors is focused primarily on their performance in concrete and concrete masonry units (CMU) as opposed to limestone, sandstone, and other historic masonry. A literature review of studies on the performance of post-installed concrete anchors, published in 1998, references over 50 studies on this topic [Cheok and Phan 1998]. Testing results and guidelines are also available for evaluating mechanical anchors in brick substrates [Brown and Borchelt 2000; BIA 1986]. Although the test set-up and protocols used in these experiments are useful to study, the anchor type studied and test results are not completely relevant to evaluating their performance in stone masonry.

Figure 2.2: Stone spall at mechanical anchors

Forsberg, Limaye and Biggs completed an in-situ test of expansion anchors to test secondary façade anchors on a particular building. A secondary anchorage system was being designed after the primary system had failed. This case, although applied to concrete, illustrates why more laboratory testing is required. The engineers specifying the anchor solution in the field did not feel comfortable endorsing a repair detail based on the test data provided by the manufacturer because they were using the anchors in a slightly different manner than specified by the manufacturer. Interestingly, the anchors, as installed, were found to be acceptable even though they were not installed to the torque values and embedment depths recommended by the manufacturer [Forsberg, Limaye and Biggs].

Technical information available from the Powers website on the various mechanical anchor systems only specifies the use of the anchors in concrete, structural lightweight concrete, grout-filled concrete block and in some cases, red brick. Although a short section on stone as a base material is included in the expanded Architects and Engineers manual (Powers Fasteners 2005), tables for allowable and ultimate loads in stone masonry along with masonry-specific installation instructions are non-existent. Product information for Powers fasteners includes performance data for these concrete materials as well as red brick (with compressive strengths greater than 1500 psi), but only includes general information on stone substrates, recommending a testing program be completed because of the wide variability of stone strength [Powers Fasteners 2005]. This reference also mentions that very large factors of safety (up to 10:1) may be used when encountering factors such as questionable base material (such as the variability of stone substrates).

The primary method for determination of published design values is a factor of safety approach. Factors of safety are divisors that are applied to the experimental average ultimate strength to allow for field conditions that invariably differ from a well-controlled lab environment. A statistical COV (Coefficient of Variation) method is mentioned

briefly as being considered for future editions of the manual as methods in Strength Design of masonry become more widely accepted in future editions of the International Building Code. The Coefficient of Variation for Mechanical Anchors is listed as between 10 - 15% [Powers Fasteners 2005]. Currently the factor of safety that is recommended for the design values in both shear and tension for both anchor types used in concrete is 4.0.

3. Methods and Materials

The first task of this study was to confirm the authors' belief that the engineering community is excessively conservative when specifying the use of mechanical anchors in stone base materials. An online survey was distributed to the preservation engineering community. A simple design problem was presented, asking for the specification of design values for a hypothetical installation.

The lab portion of the research was designed as a screening experiment to evaluate a reasonably large number of variables in order to determine which factors influence the response -- in this case the ultimate strength of the anchor installations. The ultimate goal for future research is to determine which nondestructive evaluation (NDE) variables will most accurately determine the appropriate design values for anchors installed in natural stone.

The primary (control) variables examined in this study are
1) type of stone
2) orientation of bedding planes
3) type of anchor
4) type of test; ie, tension or shear

The secondary (measured) variables are
1) pulse velocity (all specimens),
2) Schmidt hammer readings (all specimens)
3) compression tests (limited specimens).
4) failure mode (all specimens)

The next section of this report discusses each of these variables in greater detail:

Type of Stone

The experimental program utilized 10-inch cubes of both Ohio Sandstone and Indiana Limestone, fabricated and donated by Old World Stone in Burlington, Ontario. Each specimen was examined and marked with a unique specimen number and each face was marked with a face number to control for bedding orientation during comparison of anchor strength as a function of stone "grain".

Figure 3.1: Marked specimens

Orientation of Bedding Plane

The orientation of stone bedding plane relative to the axis of the bolt installation is a significant variable. Unlike concrete, limestone and sandstone are not isotropic materials, and the anchors perform differently when installed in different orientations.

For the tension tests there are only two unique bedding orientations to study: perpendicular and parallel (Figure 3.2).

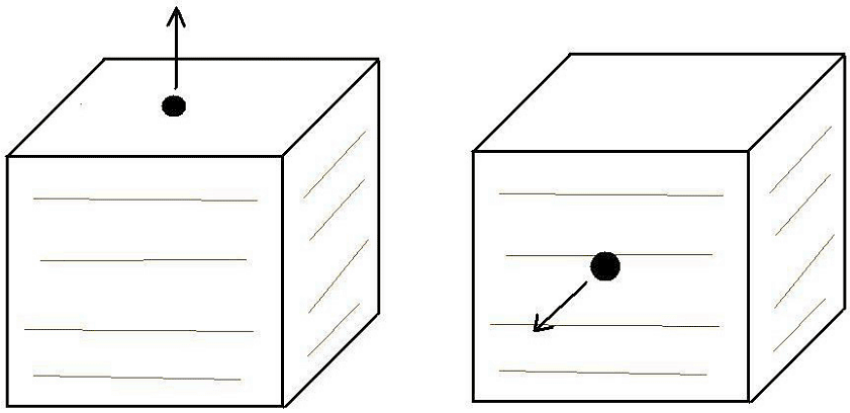

Figure 3.2: Orientation of bedding plane in tension

However, for the shear tests there are three different combinations of bedding orientation and pull direction to record. In Figure 3.3, the top two images are identical for our purposes: the bolts are installed perpendicular to the bedding plane and pulled perpendicular to the bedding plane. The lower left image shows the bolt installed parallel to the bedding plane, but pulled perpendicular to the bedding plane. Finally, the lower right image shows the anchor installed and pulled parallel to the bedding plane.

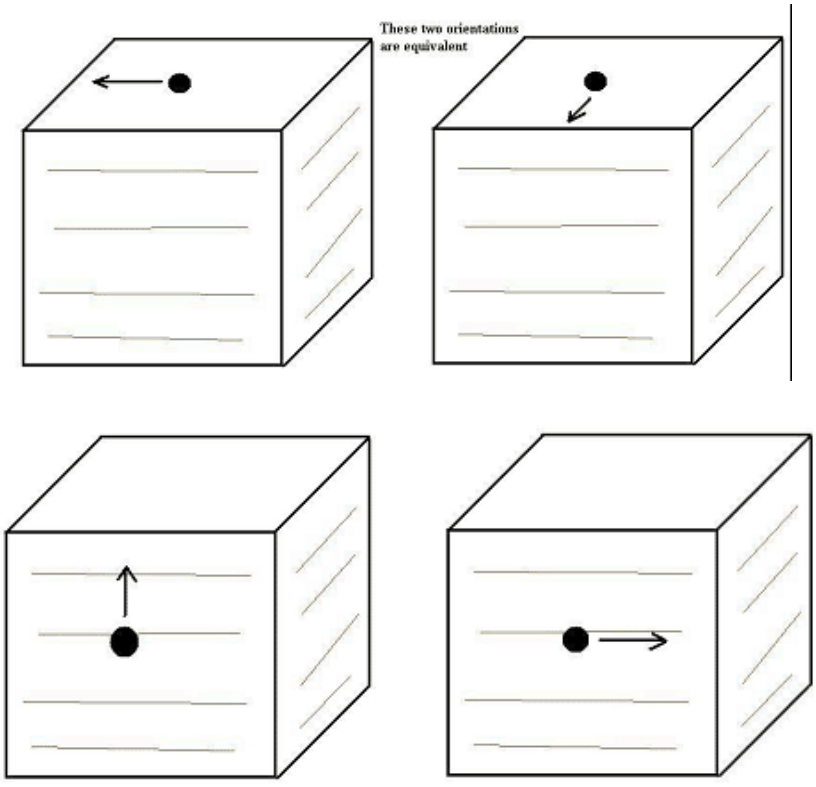

Figure 3.3: Orientation of bedding plane in shear

Type of Anchor
One mechanical anchor was installed in the center of each face of each block following the manufacturer's instructions for their installation in concrete. The Power-Stud anchors were installed with an embedment length of 2" for both the tension and shear tests; the Wedge-Bolt anchors were installed with an embedment length of 2 $^{1}/_{8}$"for the tension tests and 2 ¼" for the shear tests, following the minimum embedment recommendations listed in the specifications [Powers Fasteners 2005].

Figure 3.4: Wedge-Bolt (left) and Power-Stud (right)

Before any anchors were placed, two different nondestructive tests were undertaken, each parallel to and perpendicular to bedding orientation: Schmidt Hammer and Ultrasonic Pulse Velocity (UPV).

The Schmidt Hammer
The Schmidt Hammer consists of a spring-loaded steel mass that is automatically released against a plunger when the hammer is pressed against the specimen surface. A small

sliding pointer indicates the rebound of the hammer on a graduated scale. The test is based on the principle that the portion of the hammer's kinetic energy transferred to the stone as elastic deformation, rather than plastic deformation, will cause the hammer to rebound. The distance traveled by the hammer mass, expressed as a percentage of the initial extension of the spring, is called the Rebound Number and is a measure of the surface hardness of the material. The Schmidt Hammer test is very easy to conduct and took approximately one minute per specimen-face to complete.

Ultrasonic Pulse Velocity (UPV)
The UPV test measures the travel time of an ultrasonic pulse through a material. The basis for NDE research using ultrasonic waves is the idea that aberrations in wave propagation through a material may be studied in order to understand certain characteristics of the material. The primary characteristic of the ultrasonic pulse studied here is its velocity through the stone. There are numerous studies on ultrasonic pulse velocity in concrete [Graff 1975, 244-245].

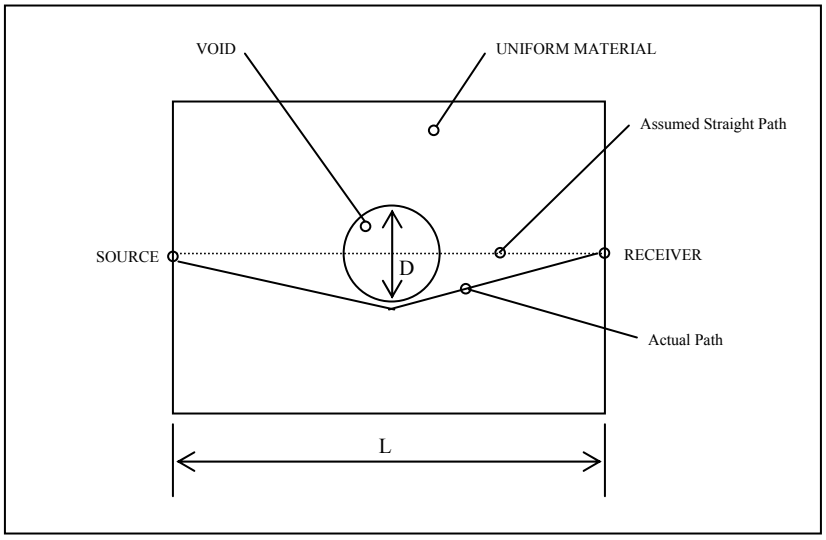

Figure 3.5 Effect of a void on pulse path length
(Adapted from Schuller and Abbaneo, 1994)

The speed at which the pulse travels can be used to determine the compressive strength of concrete. The more voids and inclusions encountered along a ray path through a material, the less dense the sample and the lower the compressive strength of the material. The ASTM document for UPV in concrete is *ASTM C597-02 Standard Test Method for Pulse Velocity through Concrete*.

The UPV measurements were taken with a combination of a hammer-mounted accelerometer and a 50 kHz transducer. All data was acquired using a National Instruments NI 6063-E data acquisition card installed in a laptop computer. Custom MATLAB routines were then used to analyze the data files to determine the travel time of

each hammer pulse. All UPV tests were taken using the direct transmission method meaning that the impulse was applied directly across the sample from the receiving transducer.

The zero-crossing method [Graff 1975, 244-245] calculates the pulse arrival time by comparing the hammer-couplant-receiver output to the hammer-specimen-couplant-receiver output. In Figure 3.6 below the green control plot shows the displacement-versus time trace for the source and receiver directly connected through a thin layer of couplant. The blue plot displayed is the signal through well-consolidated concrete. The calculation of the arrival time using the zero-crossing method is shown.

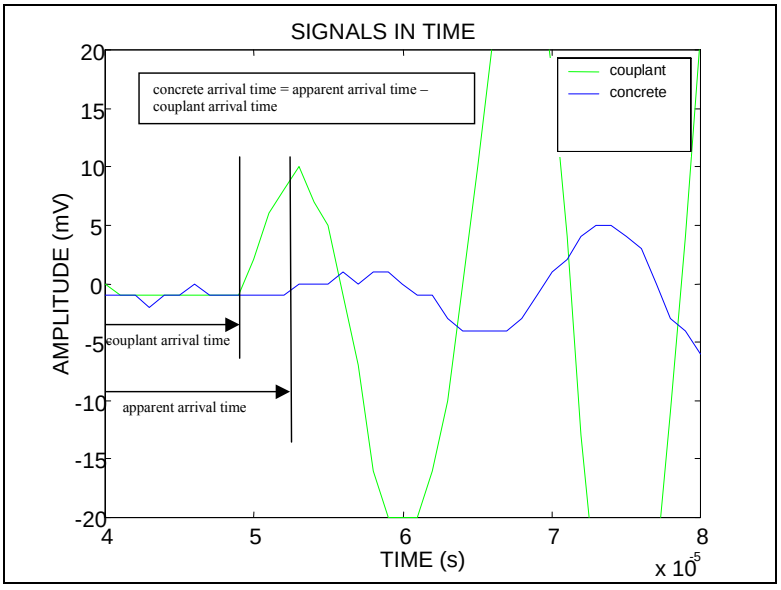

Figure 3.6: Zero-crossing method

Instron Testing Machine

For all destructive pull-out and shear tests, an Instron TTD-M1 was used in conjunction with a custom-designed and fabricated specimen testing frame.

Figure 3.7: Instron machine with testing frame

The LabJack, a USB data acquisition interface, was used to connect the load cell to a laptop computer. A Model F, Serial 508F, 10,000-pound capacity load cell was used to complete the tension and shear tests. Given the age of the load cell, careful calibration was undertaken to confirm the linearity of the load cell through 5300 lbs. The complete calibration procedure is outlined in Appendix C.

4. Results and Discussion

If in fact anchor installation performance behaves similarly in stone as in concrete, ultimate yields will be a function of the compressive strength of the base material but are subject to the strength of the bolt material. In other words, even if a base material has an infinite compressive strength, the anchor bolt itself will eventually fail. An initial goal was to determine whether the relationship between anchor installation strength and compressive strength of base material is linear below the bolt failure threshold. This theorem is derived from the published literature for design strength of the anchors. The Powers Fasteners design manual specification suggests that, "Linear interpolation may be used to determine ultimate loads for intermediate embedments and compressive strengths" [Powers Fasteners 2005]. Figure 4.1 illustrates this theory.

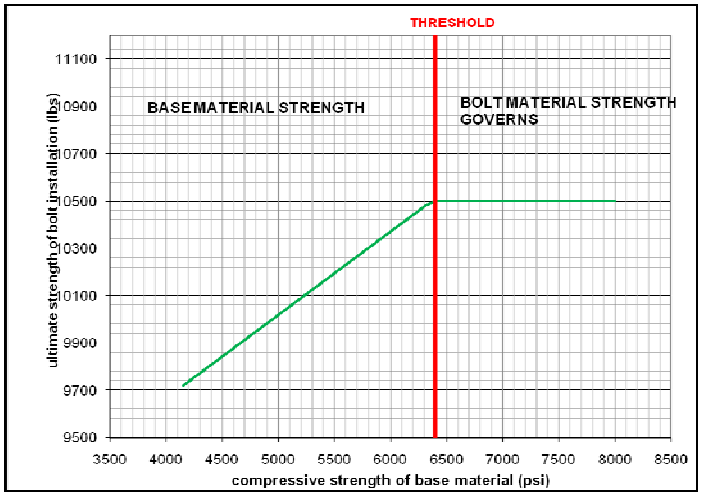

Figure 4.1: Anchor strength theorem

Engineering Judgment Survey Results
The results of the Engineering Judgment Survey showed that engineers tend to be extremely conservative when designing these anchors in tension and shear – probably due to the large variation of compressive values between and within types of natural stone. Even though the commonly accepted minimum Indiana Limestone compressive strength value is 4,000 psi [Indiana University], the designers were more likely to use the 2,000 psi concrete design value. This is even more surprising in sandstone: with an accepted average compressive strength of approximately 10,250 psi [Richardson 1917], engineers were again more likely to use the 2,000 psi concrete design value.

Given that the only method to accurately determine compressive strength of stone is destructive and since in many cases involving historic structures this is not an option, we investigated whether available nondestructive methods could be used to predict compressive strength of our samples in a controlled laboratory environment. This methodology could ultimately increase the confidence of designers in the field, allowing them to use more realistic values and therefore fewer anchors when designing these installations.

Outlier Analysis
Even the most robust experimental program will result in some anomalous data. Outliers, or data points outside a defined acceptable range, are inspected and potentially omitted from the data set. The expected range of pulse velocities in limestone and sandstone is difficult to define due to the lack of published values for pulse velocity in natural stone, and the significant variation in this property from one quarry sample to the next. In the absence of published values of pulse velocity specific to this quarry, we have applied a statistical inter-quartile [Ang and Tang, 1975] method for identifying possible outliers. These measurements were further inspected for errors in the computational method. This secondary measure resulted in the removal of just two out of a total of 127 pulse velocity readings.

Experimental Results

Failure Modes: Tension
The number of different tensile failure modes observed in the lab was unexpected and presented another significant variable to track and analyze. In addition to the more classic failure modes of large cone failure and anchor failure (Figure 4.2), four other failure modes were observed.

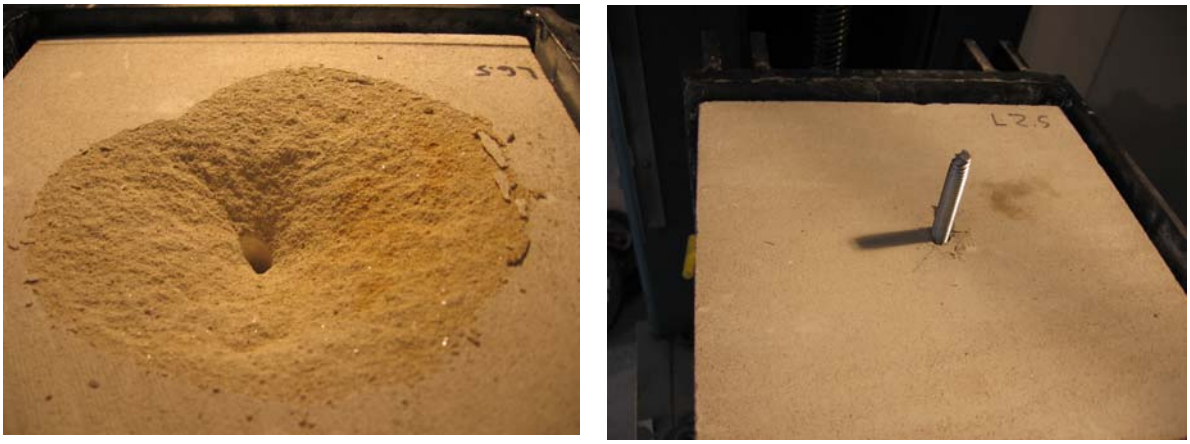

Figure 4.2: Tension failure modes: large cone (left) and anchor failure (right)

Figure 4.3 displays four of the unexpected failure modes: small cone failure (a combination of partial pull out and then cone failure), cube splitting, face delamination and bolt pull out. The varied failure modes had a significant impact on the analysis of the data, especially for the tension specimens.

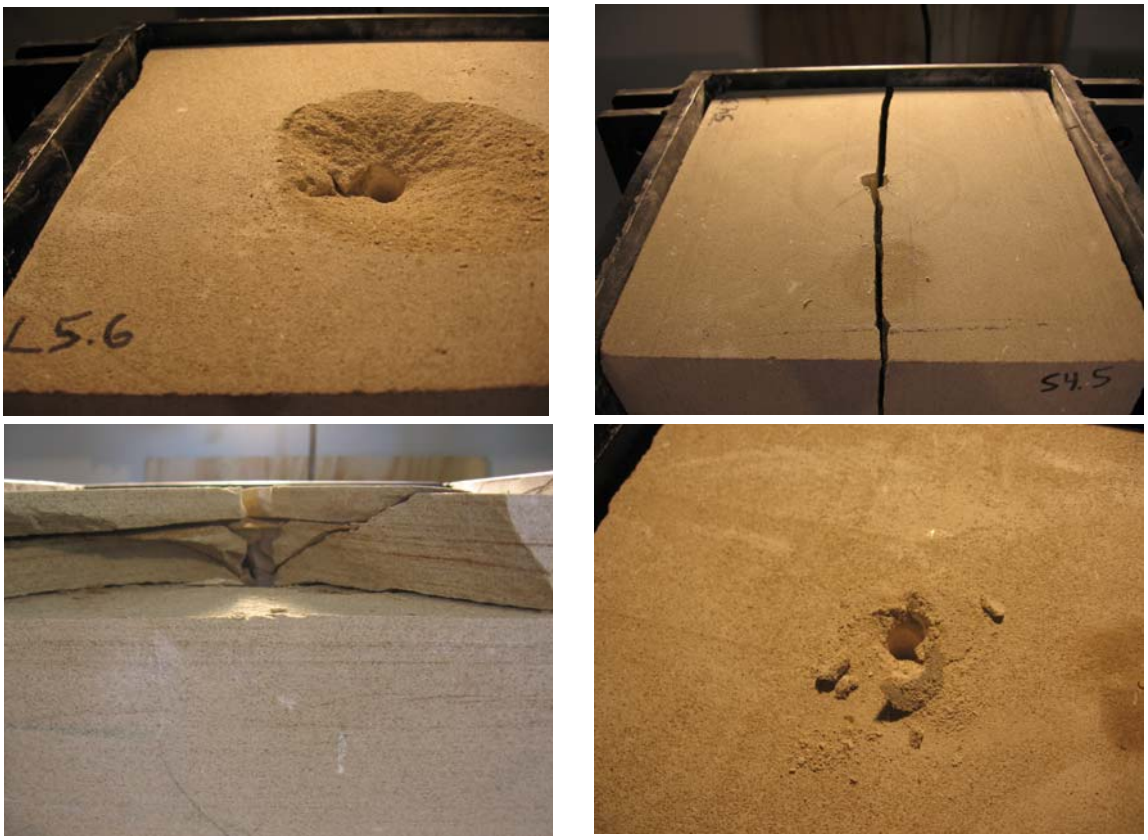

Figure 4.3: Tension failure modes: small cone (upper left), cube splitting (upper right), face delamination (lower left), anchor pull-out (lower right)

Ultimate Tension Results

The results in Table 4.1 demonstrate, with just two exceptions, that the average ultimate tension strengths of Power-Studs and Wedge-Bolts in both stone types exceed the published design strength of these bolts in 4000 psi concrete. The predominant failure mode in sandstone varies by bedding orientation with face delamination being the most common when the bolts were installed perpendicular to the bedding plane. Cube splitting and large cone failure were more common when the bolts were installed parallel to the bedding plane of the sandstone.

The failure modes were more varied among the limestone blocks. In the Power-Stud limestone specimens, bolt failure was the most common, with the bolts breaking at the threads. The anchor-to-limestone bond exceeded the material strength of the anchor in 19 of the 24 Power-Stud samples. In contrast, only 2 of the 17 Power-Stud-sandstone samples tested developed full strength of the anchor. In other words, the block failed first. It is not clear why this occurred; given sandstone's greater compressive strength, we wouldn't expect to see base material-based failure in such a large number of specimens.

Overall, the Power-Stud seems to be an excellent choice for limestone installations loaded in tension, regardless of bedding orientation. In sandstone, however, the Wedge-Bolts exhibited greater ultimate strength with lower variability between tests.

Regardless of the observed failure mode, these results suggest that the published design values in 4,000 psi concrete are appropriate, and in some cases conservative, for all variable combinations tested. This is in contrast to the study's engineering judgment survey where engineers tended to design according to the published 2,000 psi concrete values. These test results indicate that use of these design values in Indiana Limestone and Ohio Sandstone is overly conservative.

In Table 4.1, the green highlighted value illustrates the published design value that can be used to safely reflect our lab results in stone. For example, the use of the 6000psi concrete design value of 4075psi is a safe and conservative design value for a limestone Power-Stud installed parallel to the bedding plane, since we observed an average ultimate tension of 5846 lbs in the lab. In other words, 5846 lbs is greater than 4075 lbs.

TENSION TEST CONFIGURATION	Pub. Concrete Tension Strength			Specimen Tension
	2000 psi	4000 psi	6000 psi	
LIMESTONE, POWER-STUD PARALLEL	2800	3850	4075	5846
LIMESTONE, POWER-STUD, PERPENDICULAR	2800	3850	4075	5888
LIMESTONE, WEDGE-BOLT, PARALLEL	3000	3920	5200	4422
LIMESTONE, WEDGE-BOLT, PERPENDICULAR	3000	3920	5200	5029
SANDSTONE, POWER-STUD PARALLEL	2800	3850	4075	5290
SANDSTONE, POWER-STUD, PERPENDICULAR	2800	3850	4075	4730
SANDSTONE, WEDGE-BOLT, PARALLEL	3000	3920	5200	4662
SANDSTONE, WEDGE-BOLT, Perpendicular	3000	3920	5200	4002

Table 4.1: Anchor strength in tension (lbs)
Equivalent published concrete compressive strength is highlighted green

Ultimate Shear Results

The comparison of the engineering judgment survey responses and the lab results for the shear tests showed an equally conservative tendency to underestimate the ultimate shear capacity of the anchors. With the exception of two specimen configurations, highlighted in red below in Table 4.2, the lab data demonstrated that the ultimate shear strength of the bolt installations exceeds the published design values in 6000 psi concrete, whereas the engineers surveyed again chose to use the 2,000 psi concrete published value – the design value based on their installation in the lowest strength concrete.

SHEAR TEST CONFIGURATION	Pub. Concrete Shear Strength			Specimen Shear
	2000 psi	4000 psi	6000 psi	
LIMESTONE, POWERS, PARALLEL, PARALLEL	3560	3760	3760	3212
LIMESTONE, POWERS, PARALLEL, PERPENDICULAR	3560	3760	3760	4416
LIMESTONE, POWERS, PERPENDICULAR	3560	3760	3760	4511
L IMESTONE, wedge, PARALLEL, PARALLEL	4400	5080	6840	7821
LIMESTONE, wedge, PARALLEL, PERPENDICULAR	4400	5080	6840	7948
LIMESTONE, wedge, PERPENDICULAR	4400	5080	6840	7576
SANDSTONE, POWERS, PARALLEL, PARALLEL	3560	3760	3760	3866
SANDSTONE, POWERS, PARALLEL, PERPENDICULAR	3560	3760	3760	3457
SANDSTONE, POWERS, PERPENDICULAR SHEAR	3560	3760	3760	4254
SANDSTONE, WEDGE, PARALLEL, PARALLEL	4400	5080	6840	7384
SANDSTONE, WEDGE, PARALLEL, PERPENDICULAR	4400	5080	6840	8517
SANDSTONE, WEDGE, PERPENDICULAR SHEAR	4400	5080	6840	7044

Table 4.2: Anchor strength in shear (lbs)
Equivalent published concrete compressive strength is highlighted green
Tests less than published concrete class is highlighted red

From Table 4.2 we see that in both limestone and sandstone, the Wedge-Bolt is the superior choice for bolt installation in shear, with ultimate shear values exceeding the 6,000 psi design level in every installation. As expected, the Wedge-Bolts provide much greater shear strength - in some cases two or three times greater than the Power-Stud. This trend is consistent with the higher published ultimate shear values of the Wedge-Bolts in concrete.

Compressive Strength
As anticipated, the destructively-determined compressive strength of the stone is a good predictor of bolt failure in the limited number of tests performed. The selection of specimens to be tested destructively was based on the commonality of the variables, including failure mode, such that the sample diversity of specimens was maximized. Figure 4.4 shows the results of the destructive compressive strength testing. These specimens are representative of all specimen types, including bedding orientations and pull-test failure modes. When examined in total, no obvious pattern emerges from the data.

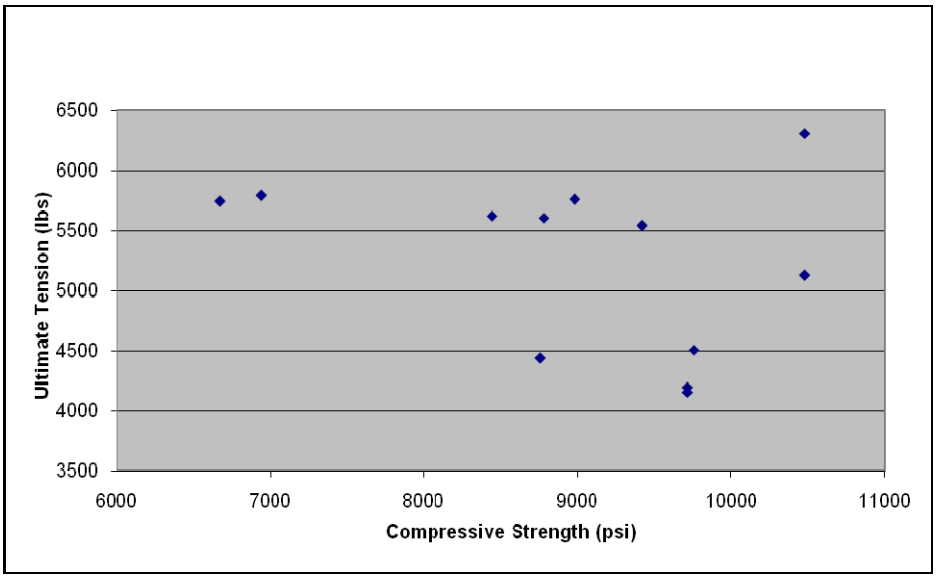

Figure 4.4: Ultimate tension vs. compressive strength for all specimens tested destructively

However, when we isolate the sandstone results, then further separate the data by failure mode of the anchor installation, we can make some valuable observations. Figure 4.5 shows all of the compressive testing results for the sandstone specimens alone.

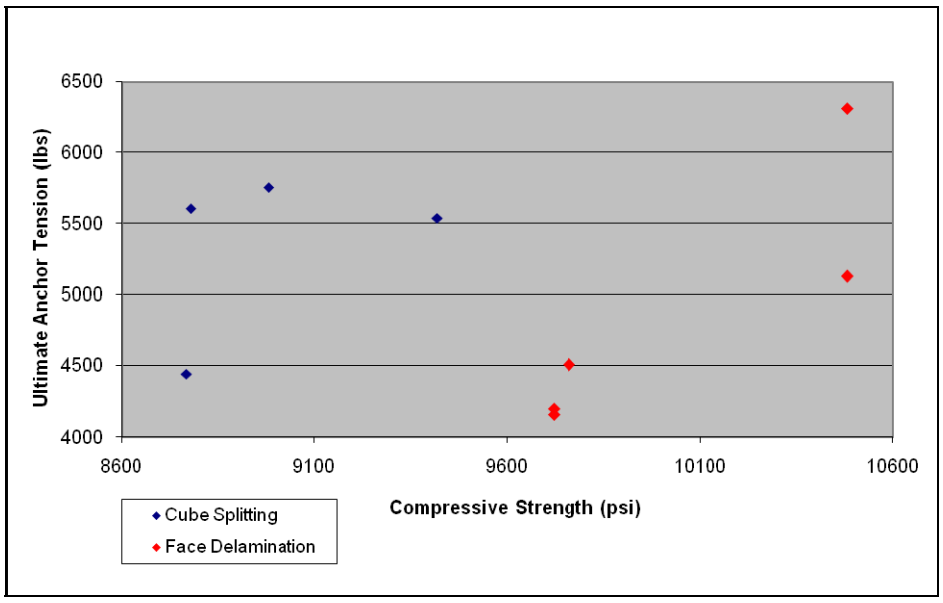

Figure 4.5: Ultimate tension vs. compressive strength for sandstone specimens tested destructively

The blue series in Figure 4.5 represents those sandstone specimens that failed because of cube splitting. Compressive strength has no correlation to the anchor tension failure in those cases where inter-laminar weakness, rather than compressive strength, governed the

failure. The red data points in Figure 4.5 show a more linear relationship for face delamination failures. The plot also shows that cube splitting is more likely when the compressive strength of the base material is lower than approximately 9600 psi, with the more classic and expected cone failure mode occurring at higher compressive strengths. Immary, inter-laminar weakness is associated with lower compressive strength.

It should be noted that some failure modes are likely confined to our laboratory and should be interpreted accordingly. For example, cube splitting is probably a result of the specimens having near-critical edge distances on all four sides, or a complete lack of edge constraint. This is an unlikely condition in the field, where individual stone units are surrounded by other units bound in a relatively soft mortar matrix.

Destructive testing was not performed on any shear test samples due to budget constraints.

Destructive testing of historic materials is obviously best avoided whenever possible, therefore pulse velocity and Schmidt hammer tests were also employed, with the hope that they would have some predictive value in determining ultimate anchor strength.

Schmidt Hammer Results

The Schmidt hammer results varied over too small a range to be a good predictor of bolt installation strength. The range of Schmidt hammer results expressed in arbitrary rebound units was 43 to 49, a 14% range, which is within 2% of the variance of the readings on individual block faces. These results caused us to dismiss this data as they are not good predictors of compressive strength.

Pulse Velocity Results - Tension

The correlation between the pulse velocity results and anchor installation strength varied significantly depending on which failure mode was exhibited by each specimen. For example, in Figure 4.6 – the pulse velocity vs ultimate tension plot for the limestone Wedge-Bolts – where anchor slippage and small cone failure were the failure modes observed, no obvious pattern is discernible. This is not surprising, since there is no reason to anticipate that compressive strength (as relatively measured by pulse velocity) is a good predictor of anchor-base material bond.

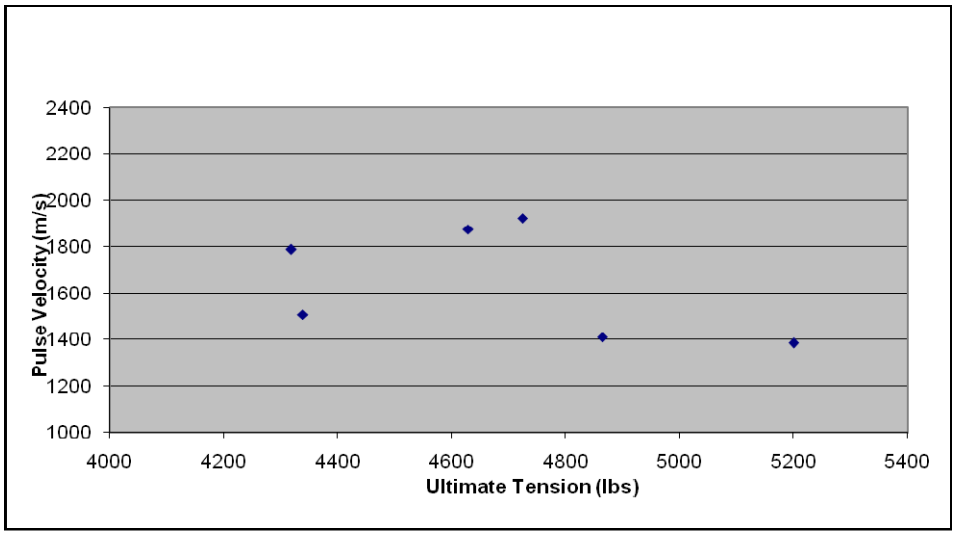

Figure 4.6: Pulse velocity vs. ultimate tension of limestone Wedge-Bolt samples

For other specimen configurations, however, we found pulse velocity to be a good predictor of compressive strength in the tests where base, rather than bolt, material properties governed the bolt system failure. Figure 4.7 shows the pulse velocity vs ultimate tension for the limestone Power-Stud (parallel to bedding) installations tested – the anticipated close-to-linear trend is observed.

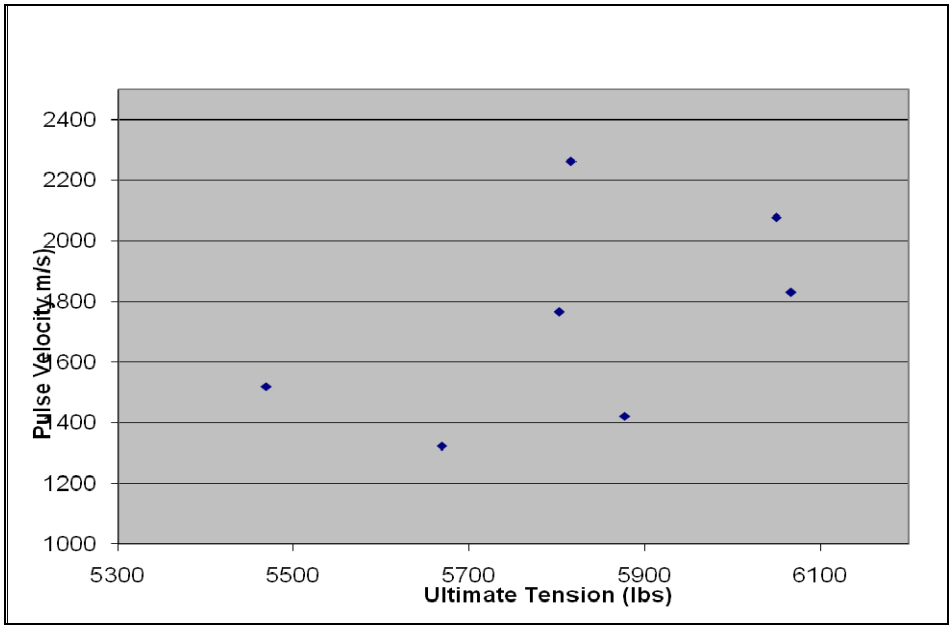

Figure 4.7: Pulse velocity vs. ultimate tension of limestone Power-Stud samples

Large cone failure was the predominant failure mode observed with six of the seven installations failing in this manner. The highest ultimate tension value occurred because

of bolt failure. More specimens with faster pulse velocities, indicating larger compressive strengths, would have to be completed in order to conclude that there is a clear threshold where base material ceases to govern the installation strength, as theorized earlier (see Figure 4.1).

Pulse Velocity Results – Shear

Unlike the tension tests where the pull direction was always along the bolt axis, the shear tests have an additional variable when the bolt is installed parallel to the bedding plane: the pull direction with respect to the bedding plane (see Figures 3.2 and 3.3). In shear tests, the pulse velocity in the direction of pull (whether parallel or perpendicular to the bedding plane) appears to be a valid predictive variable. Although faster pulse velocities generally correspond to higher compressive values, we found the higher pull-direction pulse velocities generally correlate to a *lower* ultimate shear strength. Figures 4.8 and 4.9 show the pulse velocity in the pull direction versus the ultimate shear value of the Power-Stud installations for both limestone and sandstone samples. Figure 4.8 shows those specimens where the anchor was installed perpendicular to the bedding plane.

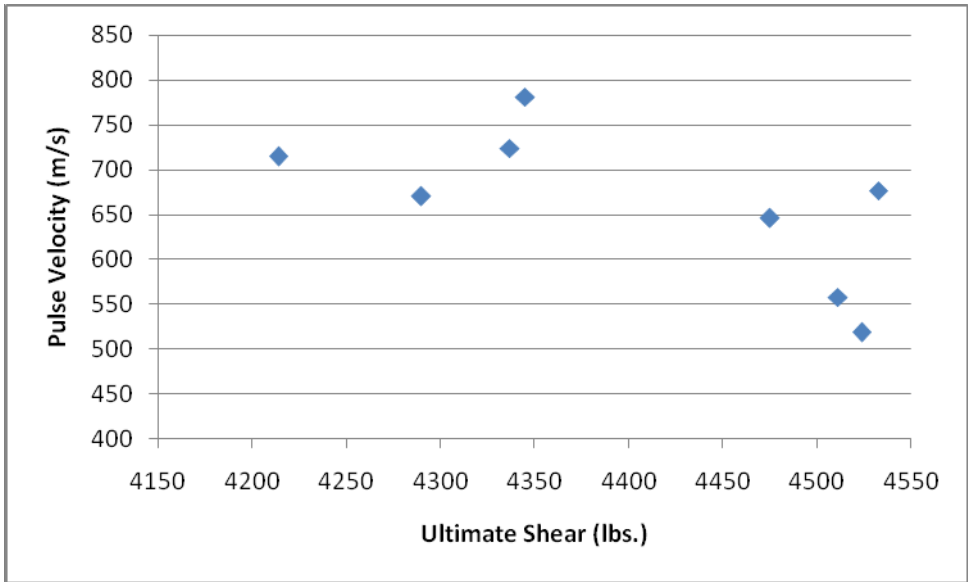

Figure 4.8: Limestone and sandstone pulse velocity (in pull direction) vs. ultimate shear for Power-Studs installed perpendicular to bedding plane

Figure 4.9 shows those where the anchor was installed parallel to the bedding plane.

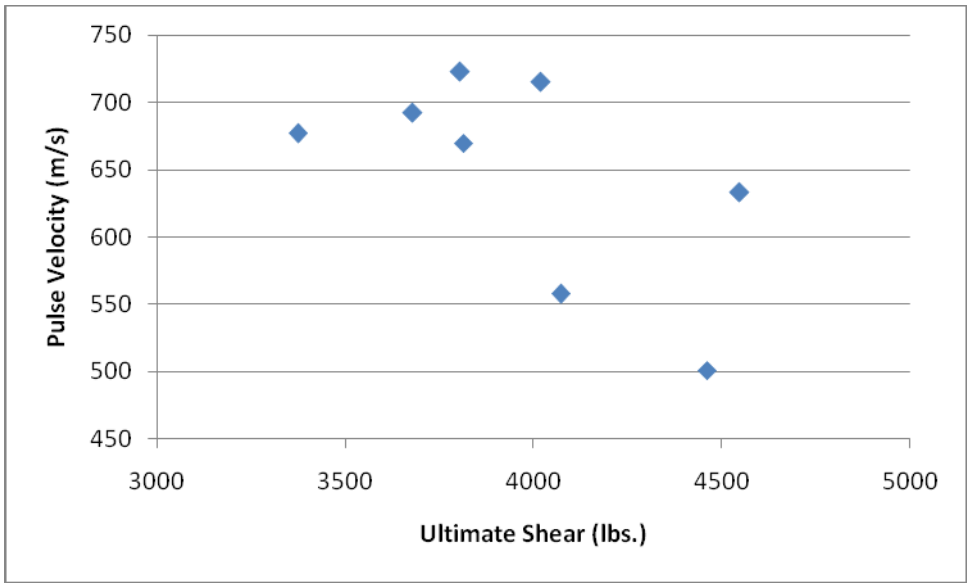

Figure 4.9: Limestone and sandstone pulse velocity (in pull direction) vs. ultimate shear for Power-Studs installed parallel to bedding plane

A simple interpretation of the data makes intuitive sense: the faster the pulse velocity in the pull direction, the fewer boundaries the energy is encountering between source and receiver. One might assume then, that faster pulse velocities correlate with lower shear capacities because the anchor can more easily initiate failure between bedding planes (similar to the splitting along wood grain). In testing however, bolt shearing, not base material failure, is the most common failure mode for the Power-Studs in shear.

A more enlightened way to consider the results is that the tests were designed to study the bolt installations in pure shear. In reality, however, the failure of the bolts was a combination of shear and bending; the closer we were to pure shear, the higher the ultimate capacity of the installation. When the bolt initially moves and starts to displace the base material (because of the easier path when pulling parallel to the bedding plan), the bolt begins to experience bending near the surface of the block, in addition to shear. Bolts then fail at a lower ultimate load because of the combined loading on the steel anchor. Figure 4.10 illustrates this theory.

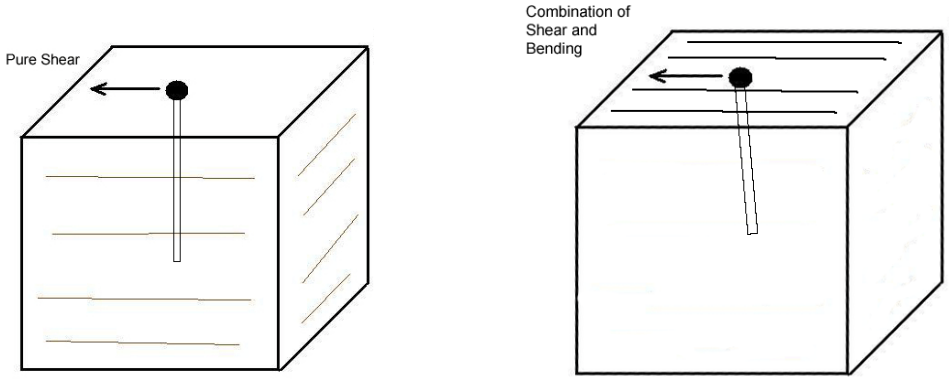

Figure 4.10: Illustration showing difference between pure shear test (on the left) and combination of shear and bending (on the right)

The Wedge-Bolt samples showed a similar trend although at much higher ultimate strengths than the Power-Studs. In both the sandstone and limestone samples, the ultimate strength of the bolt installations exhibited an inversely proportional relationship to the pulse velocity in the pull direction, as demonstrated in Figures 4.11 and 4.12.

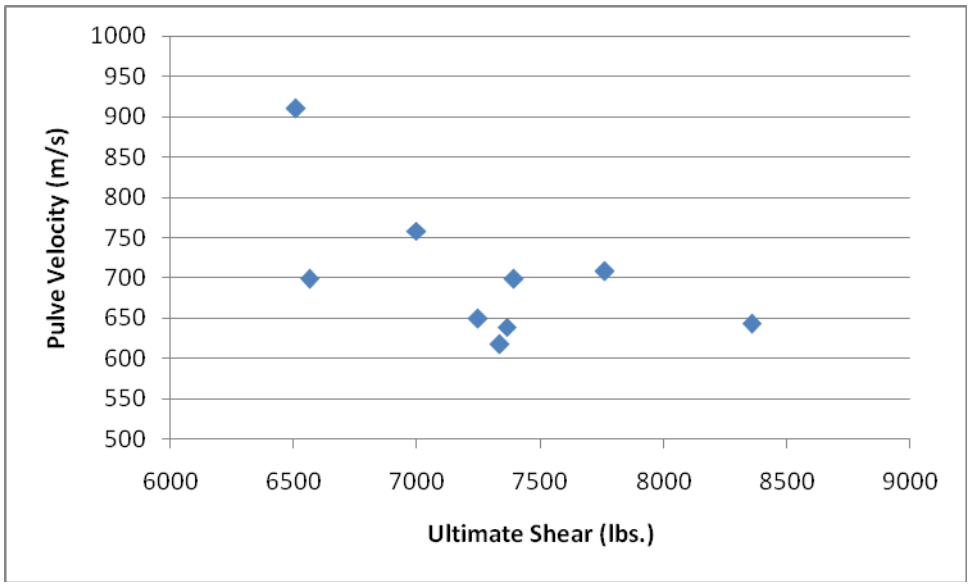

Figure 4.11: Limestone and sandstone pulse velocity (pull direction) vs. ultimate shear for Wedge-Bolts installed perpendicular to bedding plane

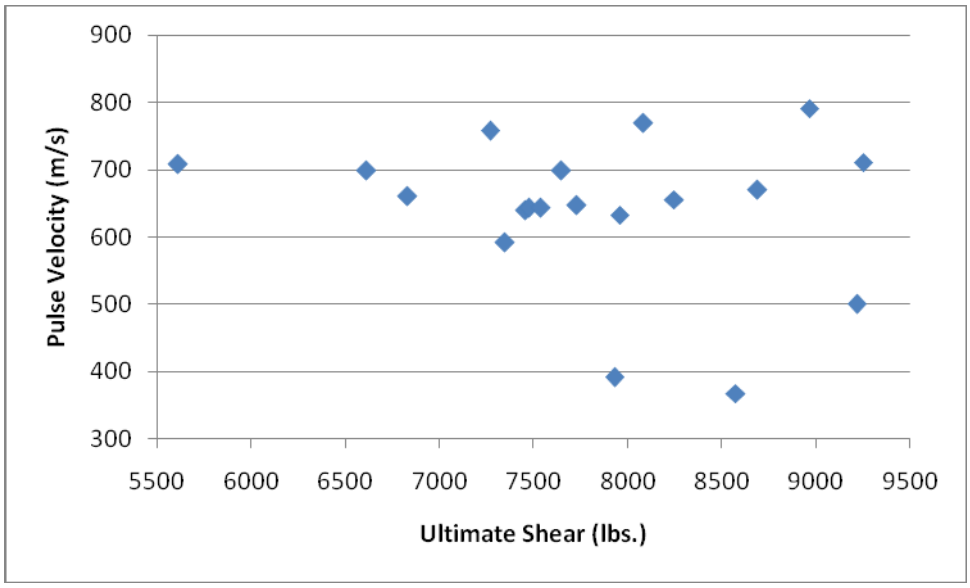

Figure 4.12: Limestone and sandstone pulse velocity (pull direction) vs. ultimate shear for Wedge-Bolts installed parallel to bedding plane

5. Conclusions

The pulse velocity data showed promise for further research in attempting to predict ultimate tension and shear installation strengths regardless of bolt and stone type. One promising opportunity for further research is to study limestone and sandstone samples from different sources with compressive strengths that vary more. The results would cover more range and increase our confidence in the apparent linear and possibly predictive trends.

The Schmidt hammer results did not have any predictive value for the shear and tension ultimate strengths regardless of bolt used, base material or bedding plane orientation. The surface hardness of natural stone, as tested using the Schmidt hammer test was not an accurate measure of the compressive strength of the sample.

The results of the Engineering Judgment Survey confirm that the engineering community tends to be overly conservative when designing these anchors in natural stone materials.

The overall performance of the anchors in limestone and sandstone was impressive. In tension, the Power-Stud proved to be an excellent choice for both Indiana Limestone and Ohio Sandstone installations, with capacities exceeding the 6000psi concrete designated values. In shear, the Wedge-Bolts exceeded the 6000psi concrete design values in all Indiana Limestone and Ohio Sandstone installations, regardless of bedding orientation and pull direction.

In conclusion, a more concentrated pulse velocity research project, with greater base material variation would likely yield a clear design approach. The pulse velocity test would be easily implemented in the field and would not require destructive tests to historic

masonry. The resulting increased design values for anchor installations in natural stone would increase the spacing of the bolts, ultimately reducing damage to historic facades.

Experimental Design Drawbacks

The main flaw of the experimental design of the research was the use of such small stone cube samples. The decision to use the 10" samples size was driven primarily by a desire to maintain critical edge distances while maintaining manageable sample sizes.

Although the minimum edge distances were maintained by using 10" cubes, the published ultimate strengths of the anchors in concrete do not mention the case where those critical edge distances are realized in all four directions – an unlikely condition in the field. As illustrated by the photos in Figure 5.1, edge distances did determine the failure mode observed on several samples. If edge distances had been greater, we anticipate a different failure mode and higher ultimate strength values in the samples where cube splitting was observed. This would have increased our sample size of meaningful data.

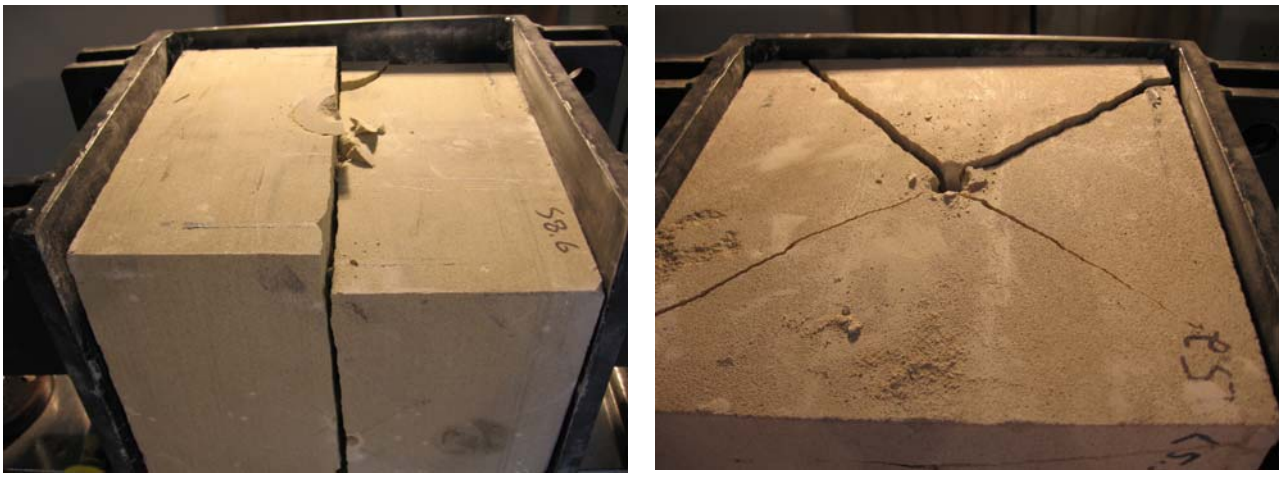

Figure 5.1: Sandstone specimens that failed by cube splitting

Topics for Further Research
The results of the various screening variables are summarized in Table 5.1.

Variable	**Results**	**Recommendations for Future Research**
Type of Stone	The assumption that the compressive strength of the base material would have a direct effect on the tension and, to some extent, shear capacities of the installations was proven *within* a substrate type only.	The concern is that some of these conclusions may not be valid because of the unanticipated failure modes observed. When the mode of failure is considered, the compressive strength of the material does have a nearly linear relationship with the ultimate tension strength of the installation. Increasing the sample dimensions would reduce the occurrence of cube splitting, an unlikely failure mode in the field.
Bedding Orientation	In every case, the performance of the installations differed by bedding orientation. Notably, the predominant failure mode was dependent on bedding orientation.	In any research program going forward, the bedding orientation must be tracked. In the field, determining the bedding orientation of the natural stone in a wall installation is typically straightforward.
Type of Anchor	Of the two anchors tested, the Power-Stud proved to be an excellent choice for both limestone and sandstone tension applications, regardless of bedding orientation. In these cases the anchors should be designed using the 6000 psi concrete design value. In shear, the conclusion for the Power-Stud is not as clear, regardless of bedding orientation and direction of pull. However, the Wedge-Bolts exceeded the 6000 psi design level in concrete.	Power-Studs and Wedge-Bolts were chosen for the research because they represent two different types of mechanical anchors: expansion-type and screw-type. The installation of the Wedge-Bolt is simpler and the Wedge-Bolts are easier to remove — a significant factor for façade applications. The specification of the Power-Stud for tension applications must take into account the more difficult removal process, potentially resulting in more damage to the façade for temporary installations.

Type of Test	Both testing procedures worked well with the tension rig testing in pure tension and the shear testing in pure shear at the anchor/specimen plane.	In the field, the more likely loading condition of the anchor installations is a combination of tension and shear. Future research should investigate this condition. The ultimate goal should be to arrive at an acceptable interaction equation for this loading condition. An appropriate starting point is the interaction equation published in the Powers design manual for concrete applications: $(N_u/N_n)^{5/3} + (V_u/V_n)^{5/3} \leq 1$ OR $(N_u/N_n) + (V_u/V_n) \leq 1$ where Nu= applied service tension load Nn = allowable tension load Vu = applied service shear load Vn = allowable shear load [Powers Fasteners, 2005]
Pulse Velocity	The UPV data was relatively time consuming to collect because of the experimental setup used. Because the arrival times were calculated using software with preset thresholds, we are confident that the pulse velocity readings are accurate.	Because each Ultrasonic waveform was saved and later analyzed, the process for the two bedding orientations of each specimen, collecting the data was time consuming. Future research should concentrate on evaluating commercially-available UPV testing equipment for one-sided field applications.
Schmidt Hammer	The Schmidt hammer results were not found to be a valuable indicator of either compressive strength or ultimate strength of anchor installation.	It is not recommended that the Schmidt hammer or any other surface hardness test be further evaluated.
Compressive Strength	The compressive strength showed promising results in this research.	The only testing method available to accurately determine compressive strength is destructive. Future research should concentrate on non-destructive methods (such as UPV) for predictive modeling

Failure Mode	The multiple failure modes observed in the research made analysis of the results more difficult.	The specimen sizes in future research projects should be larger to avoid having close-to-critical edge distances on all four sides of a specimen. A field testing program should also be designed in order to reduce the failure modes to those that would be realistically encountered in field situations.

Table 5.1: Screening variable results

ACKNOWLEDGMENTS

The authors would like to acknowledge the support of the National Center for Preservation Technology and Training (NCPTT), which supported the research through the PTT Grants Program.

Atkinson-Noland & Associates provided guidance and the compressive strength testing for the study. Michael Schuller, specifically, helped to edit this report and provided valuable suggestions.

Old World Stone fabricated and donated the stone specimens for the research.

Vertical Access LLC also supported the research by providing lab equipment, space and the time of Kent Diebolt to direct the research.

TABLE OF REFERENCES

1. Ang, A.H.S. and Tang, Wilson H. 1975. *Probability Concepts in Engineering Planning and Design*, John Wiley and Sons.
2. Architectural and Engineering Specification and Design Manual, Anchoring and Fastening Systems, 5th Edition
3. ASTM International. 2003. E488-96(2003) Standard Test Methods for Strength in Anchors in Concrete and Masonry Elements.
4. Brick Institute of America. 1996. Technical Notes 44: Anchor Bolts for Brick Masonry. Reston, VA: Brick Institute of America, http://www.bia.org/BIA/technotes/t44.htm.
5. Brown, Russell H. and J. Gregg Borchlt. 2000. Strength of Anchor Bolts in the Top of Clay Masonry Walls. *Council for Masonry Research Report* 12, no. 1 (Spring 2000), http://www.masonryresearch.org/CMR_Reports/cmrv12n1.pdf.
6. Building Stones and Clays: A Handbook for Architects and Engineers By Charles Henry Richardson, 1917.
7. Cheok, Geraldine and Long T. Phan. 1998. "Post-Installed Anchors-A Literature Review" NISTIR 6096. Gaithersburg, MD: Building and Fire Research Laboratory, National Institute of Standards and Technology, http://fire.nist.gov/bfrlpubs/build98/art054.html.
8. Forsberg, Thomas E., Hermant. S. Limaye and David T. Biggs. "In-Situ Testing of Expansion Anchors Embedded in Concrete."
9. Graff, K.F., Wave Motion in Elastic Solids, 1975, pp.244 - 245, Oxford University Press
10. Hilti Corporation. 2005. http://www.us.hilti.com/holus/modules/prcat/prca_navigation.jsp?OID=-12132.
11. Indiana University. http://igs.indiana.edu/geology/minRes/indianaLimestone/index.cfm
12. International Code Council. 2001. Appendix A, Guidelines for Seismic Retrofit of Existing Buildings (GSREB) in 2003 International Existing Building Code.
13. ICC Evaluation Services. 2005. Acceptance Criteria for Expansion Anchors in Concrete and Masonry Elements, http://www.icc-es.org/criteria/pdf_files/ac01.pdf.
14. Jarvis, Alan and Joffrey Hyman. 2000. Soft Sandstone Rock Anchor Testing at Swinburne, http://www.saclimb.co.za/softsandstone_report.html.
15. Powers Fasteners. 2005. http://www.powers.com/product_07246.html.

APPENDIX A: TENSION RESULTS

Stone Type	Bolt Type	Bolt Loading	Bolt:Bedding	Pull Direction	Cube #	Face #	Approx. Yield (lbs)	Maximum (lbs)	Failure Mode
Limestone	3/8" Powers Power Stud	Tension	Parallel	Normal to face	4	5	2480	5453	Bolt broke at threads
Limestone	3/8" Powers Power Stud	Tension	Parallel	Normal to face	4	6	2570	5743	Large cone
Limestone	3/8" Powers Power Stud	Tension	Parallel	Normal to face	4	3	2840	5594	Large cone
Limestone	3/8" Powers Power Stud	Tension	Parallel	Normal to face	4	4	2670	5486	Large cone
Limestone	3/8" Powers Power Stud	Tension	Parallel	Normal to face	3	6	3520	5816	Bolt broke at threads
Limestone	3/8" Powers Power Stud	Tension	Parallel	Normal to face	3	5	3280	5877	Cube split in half
Limestone	3/8" Powers Power Stud	Tension	Parallel	Normal to face	2	5	3930	6284	Bolt broke at threads
Limestone	3/8" Powers Power Stud	Tension	Parallel	Normal to face	2	6	3280	5712	Bolt broke at threads
Limestone	3/8" Powers Power Stud	Tension	Parallel	Normal to face	2	3	3280	5894	Bolt broke at threads
Limestone	3/8" Powers Power Stud	Tension	Parallel	Normal to face	2	4	3390	5747	Bolt broke at threads
Limestone	3/8" Powers Power Stud	Tension	Parallel	Normal to face	1	4	3460	6275	Bolt broke at threads
Limestone	3/8" Powers Power Stud	Tension	Parallel	Normal to face	1	6	3500	5790	Bolt broke at threads
Limestone	3/8" Powers Power Stud	Tension	Parallel	Normal to face	1	5	3490	5825	Bolt broke at threads
Limestone	3/8" Powers Power Stud	Tension	Parallel	Normal to face	1	3	3380	6344	Bolt broke at threads
Limestone	3/8" Powers Wedge Bolt	Tension	Parallel	Normal to face	8	4	2040	3221	Slipped out
Limestone	3/8" Powers Wedge Bolt	Tension	Parallel	Normal to face	8	5	2482	3871	Small cone & slippage
Limestone	3/8" Powers Wedge Bolt	Tension	Parallel	Normal to face	8	3	2690	4318	Slipped out
Limestone	3/8" Powers Wedge Bolt	Tension	Parallel	Normal to face	7	4	3800	4587	Slipped out
Limestone	3/8" Powers Wedge Bolt	Tension	Parallel	Normal to face	7	5	4260	4409	Slipped out
Limestone	3/8" Powers Wedge Bolt	Tension	Parallel	Normal to face	7	6	4200	4691	Slipped out
Limestone	3/8" Powers Wedge Bolt	Tension	Parallel	Normal to face	7	3	Unable to discern	4287	Slipped out
Limestone	3/8" Powers Wedge Bolt	Tension	Parallel	Normal to face	6	5	Unable to discern	4708	Small cone & slippage
Limestone	3/8" Powers Wedge Bolt	Tension	Parallel	Normal to face	6	6	5100	5200	Slipped out
Limestone	3/8" Powers Wedge Bolt	Tension	Parallel	Normal to face	6	4	3850	5022	Slipped out
Limestone	3/8" Powers Wedge Bolt	Tension	Parallel	Normal to face	5	6	2800	3987	Large cone
Limestone	3/8" Powers Wedge Bolt	Tension	Parallel	Normal to face	5	4	5280	5453	Slipped out
Limestone	3/8" Powers Wedge Bolt	Tension	Parallel	Normal to face	5	3	2500	4194	Slipped out
Limestone	3/8" Powers Wedge Bolt	Tension	Parallel	Normal to face	5	5	Unable to discern	3995	Slipped out
Limestone	3/8" Powers Power Stud	Tension	Perpendicular	Normal to face	2	1	3500	5573	Bolt broke at threads
Limestone	3/8" Powers Power Stud	Tension	Perpendicular	Normal to face	2	2	3240	5591	Bolt broke at threads
Limestone	3/8" Powers Power Stud	Tension	Perpendicular	Normal to face	4	1	3500	5929	Bolt broke at threads
Limestone	3/8" Powers Power Stud	Tension	Perpendicular	Normal to face	4	2	4250	6838	Bolt broke at threads
Limestone	3/8" Powers Power Stud	Tension	Perpendicular	Normal to face	1	1	3700	6301	Bolt broke at threads
Limestone	3/8" Powers Power Stud	Tension	Perpendicular	Normal to face	1	2	3700	5781	Bolt broke at threads
Limestone	3/8" Powers Power Stud	Tension	Perpendicular	Normal to face	10	1	3500	6330	Bolt broke at threads
Limestone	3/8" Powers Power Stud	Tension	Perpendicular	Normal to face	17	2	Unable to discern	4499	Face delamination
Limestone	3/8" Powers Power Stud	Tension	Perpendicular	Normal to face	12	1	4900	5691	Bolt broke at threads
Limestone	3/8" Powers Power Stud	Tension	Perpendicular	Normal to face	12	2	5000	6347	Bolt broke at threads
Limestone	3/8" Powers Wedge Bolt	Tension	Perpendicular	Normal to face	8	1	3110	3754	Large cone
Limestone	3/8" Powers Wedge Bolt	Tension	Perpendicular	Normal to face	8	2	3281	4491	Small cone & slippage
Limestone	3/8" Powers Wedge Bolt	Tension	Perpendicular	Normal to face	7	1	Unable to discern	4587	Slipped out
Limestone	3/8" Powers Wedge Bolt	Tension	Perpendicular	Normal to face	7	2	Unable to discern	5088	Slipped out
Limestone	3/8" Powers Wedge Bolt	Tension	Perpendicular	Normal to face	6	1	3750	4638	Large cone
Limestone	3/8" Powers Wedge Bolt	Tension	Perpendicular	Normal to face	6	2	Unable to discern	4456	Large cone
Limestone	3/8" Powers Wedge Bolt	Tension	Perpendicular	Normal to face	5	1	2790	5386	Slipped out
Limestone	3/8" Powers Wedge Bolt	Tension	Perpendicular	Normal to face	5	2	5180	5481	Face delamination
Limestone	3/8" Powers Wedge Bolt	Tension	Perpendicular	Normal to face	9	2	Unable to discern	6116	Face delamination
Limestone	3/8" Powers Wedge Bolt	Tension	Perpendicular	Normal to face	10	2	Unable to discern	6356	Face delamination
Sandstone	3/8" Powers Power Stud	Tension	Parallel	Normal to face	4	3	3800	4439	Cube split in half
Sandstone	3/8" Powers Power Stud	Tension	Parallel	Normal to face	3	6	3250	4389	Cube split in half
Sandstone	3/8" Powers Power Stud	Tension	Parallel	Normal to face	37	5	5400	5757	Cube split in half
Sandstone	3/8" Powers Power Stud	Tension	Parallel	Normal to face	29	4	5100	5606	Cube split in half
Sandstone	3/8" Powers Power Stud	Tension	Parallel	Normal to face	28	4	5400	6101	Bolt broke at threads
Sandstone	3/8" Powers Power Stud	Tension	Parallel	Normal to face	19	4	5100	5547	Bolt broke at threads
Sandstone	3/8" Powers Power Stud	Tension	Parallel	Normal to face	28	5	5100	5623	Cube split in half
Sandstone	3/8" Powers Power Stud	Tension	Parallel	Normal to face	19	6	4900	5539	Cube split in half
Sandstone	3/8" Powers Power Stud	Tension	Parallel	Normal to face	28	3	2600	4633	Cube split in half
Sandstone	3/8" Powers Wedge Bolt	Tension	Parallel	Normal to face	8	4	3050	5253	Face delamination
Sandstone	3/8" Powers Wedge Bolt	Tension	Parallel	Normal to face	8	3	Unable to discern	4837	Face delamination
Sandstone	3/8" Powers Wedge Bolt	Tension	Parallel	Normal to face	8	6	4030	4785	Cube split in half
Sandstone	3/8" Powers Wedge Bolt	Tension	Parallel	Normal to face	7	3	4460	5019	Face delamination
Sandstone	3/8" Powers Wedge Bolt	Tension	Parallel	Normal to face	7	4	2793	4214	Face delamination
Sandstone	3/8" Powers Wedge Bolt	Tension	Parallel	Normal to face	7	5	3890	3945	Large cone
Sandstone	3/8" Powers Wedge Bolt	Tension	Parallel	Normal to face	7	6	2850	4309	Large cone
Sandstone	3/8" Powers Wedge Bolt	Tension	Parallel	Normal to face	27	4	4100	4524	Large cone
Sandstone	3/8" Powers Wedge Bolt	Tension	Parallel	Normal to face	27	3	Unable to discern	4703	Large cone
Sandstone	3/8" Powers Wedge Bolt	Tension	Parallel	Normal to face	27	6	Unable to discern	5035	Face delamination
Sandstone	3/8" Powers Power Stud	Tension	Perpendicular	Normal to face	2	1	3130	4811	Face delamination
Sandstone	3/8" Powers Power Stud	Tension	Perpendicular	Normal to face	2	2	3000	3489	Face delamination
Sandstone	3/8" Powers Power Stud	Tension	Perpendicular	Normal to face	1	1	3100	4195	Face delamination
Sandstone	3/8" Powers Power Stud	Tension	Perpendicular	Normal to face	1	2	2720	4154	Face delamination
Sandstone	3/8" Powers Power Stud	Tension	Perpendicular	Normal to face	18	2	3100	5128	Face delamination
Sandstone	3/8" Powers Power Stud	Tension	Perpendicular	Normal to face	24	1	3200	4507	Face delamination
Sandstone	3/8" Powers Power Stud	Tension	Perpendicular	Normal to face	18	1	4900	6311	Face delamination
Sandstone	3/8" Powers Power Stud	Tension	Perpendicular	Normal to face	24	2	3500	5262	Face delamination
Sandstone	3/8" Powers Wedge Bolt	Tension	Perpendicular	Normal to face	6	1	3320	3876	Face delamination
Sandstone	3/8" Powers Wedge Bolt	Tension	Perpendicular	Normal to face	6	2	2970	3503	Face delamination
Sandstone	3/8" Powers Wedge Bolt	Tension	Perpendicular	Normal to face	5	1	2330	3945	Large cone
Sandstone	3/8" Powers Wedge Bolt	Tension	Perpendicular	Normal to face	5	2	1870	2957	Face delamination
Sandstone	3/8" Powers Wedge Bolt	Tension	Perpendicular	Normal to face	27	2	2900	3255	Face delamination
Sandstone	3/8" Powers Wedge Bolt	Tension	Perpendicular	Normal to face	27	1	Unable to discern	4280	Face delamination
Sandstone	3/8" Powers Wedge Bolt	Tension	Perpendicular	Normal to face	31	1	2800	5111	Face delamination
Sandstone	3/8" Powers Wedge Bolt	Tension	Perpendicular	Normal to face	31	2	2900	4540	Large cone
Sandstone	3/8" Powers Wedge Bolt	Tension	Perpendicular	Normal to face	38	2	Unable to discern	4305	Face delamination
Sandstone	3/8" Powers Wedge Bolt	Tension	Perpendicular	Normal to face	38	2	2800	4272	Face delamination

APPENDIX B: SHEAR RESULTS

Limestone	3/8" Powers Power Stud	Shear	Parallel	Parallel to Bedding	11	5	2500	3770	Limestone
Limestone	3/8" Powers Power Stud	Shear	Parallel	Parallel to Bedding	11	6	Unable to discern	2989	Limestone
Limestone	3/8" Powers Power Stud	Shear	Parallel	Parallel to Bedding	11	3	Unable to discern	2628	Limestone
Limestone	3/8" Powers Power Stud	Shear	Parallel	Parallel to Bedding	11	4	2450	2830	Limestone
Limestone	3/8" Powers Power Stud	Shear	Parallel	Parallel to Bedding	21	3	2700	3341	Limestone
Limestone	3/8" Powers Power Stud	Shear	Parallel	Parallel to Bedding	21	4	2500	3265	Limestone
Limestone	3/8" Powers Power Stud	Shear	Parallel	Parallel to Bedding	21	5	2300	3433	Limestone
Limestone	3/8" Powers Power Stud	Shear	Parallel	Parallel to Bedding	21	6	2500	3451	Limestone
Limestone	3/8" Powers Power Stud	Shear	Parallel	Parallel to Bedding	20	5	2600	3375	Limestone
Limestone	3/8" Powers Power Stud	Shear	Parallel	Parallel to Bedding	20	6	2100	3036	Limestone
Limestone	3/8" Powers Wedge Bolt	Shear	Parallel	Parallel to Bedding	15	6	Unable to discern	7957	Limestone
Limestone	3/8" Powers Wedge Bolt	Shear	Parallel	Parallel to Bedding	19	6	6300	8246	Limestone
Limestone	3/8" Powers Wedge Bolt	Shear	Parallel	Parallel to Bedding	16	4	Unable to discern	7545	Limestone
Limestone	3/8" Powers Wedge Bolt	Shear	Parallel	Parallel to Bedding	16	6	Unable to discern	7380	Limestone
Limestone	3/8" Powers Wedge Bolt	Shear	Parallel	Parallel to Bedding	16	5	Unable to discern	9375	Limestone
Limestone	3/8" Powers Wedge Bolt	Shear	Parallel	Parallel to Bedding	22	5	Unable to discern	7554	Limestone
Limestone	3/8" Powers Wedge Bolt	Shear	Parallel	Parallel to Bedding	22	6	Unable to discern	7454	Limestone
Limestone	3/8" Powers Wedge Bolt	Shear	Parallel	Parallel to Bedding	22	4	Unable to discern	7612	Limestone
Limestone	3/8" Powers Wedge Bolt	Shear	Parallel	Parallel to Bedding	22	3	Unable to discern	7280	Limestone
Limestone	3/8" Powers Power Stud	Shear	Parallel	Perpindicular to Bedding	12	3	3800	4152	Bolt sheared
Limestone	3/8" Powers Power Stud	Shear	Parallel	Perpindicular to Bedding	12	5	3500	4314	Bolt sheared
Limestone	3/8" Powers Power Stud	Shear	Parallel	Perpindicular to Bedding	12	4	3700	4203	Bolt sheared
Limestone	3/8" Powers Power Stud	Shear	Parallel	Perpindicular to Bedding	10	3	3950	4477	Bolt sheared
Limestone	3/8" Powers Power Stud	Shear	Parallel	Perpindicular to Bedding	10	4	3800	4383	Bolt sheared
Limestone	3/8" Powers Power Stud	Shear	Parallel	Perpindicular to Bedding	10	5	3700	4480	Bolt sheared
Limestone	3/8" Powers Power Stud	Shear	Parallel	Perpindicular to Bedding	10	6	4300	4614	Bolt sheared
Limestone	3/8" Powers Power Stud	Shear	Parallel	Perpindicular to Bedding	20	3	3900	4480	Bolt sheared
Limestone	3/8" Powers Power Stud	Shear	Parallel	Perpindicular to Bedding	18	6	3900	4592	Bolt sheared
Limestone	3/8" Powers Power Stud	Shear	Parallel	Perpindicular to Bedding	18	3	3100	4500	Bolt sheared
Limestone	3/8" Powers Wedge Bolt	Shear	Parallel	Perpindicular to Bedding	20	4	7550	9217	Instron Overloaded
Limestone	3/8" Powers Wedge Bolt	Shear	Parallel	Perpindicular to Bedding	13	3	Unable to discern	7126	Test stopped*
Limestone	3/8" Powers Wedge Bolt	Shear	Parallel	Perpindicular to Bedding	13	4	Unable to discern	7319	Test stopped*
Limestone	3/8" Powers Wedge Bolt	Shear	Parallel	Perpindicular to Bedding	13	5	Unable to discern	7596	Test stopped*
Limestone	3/8" Powers Wedge Bolt	Shear	Parallel	Perpindicular to Bedding	13	6	7800	8064	Test stopped*
Limestone	3/8" Powers Wedge Bolt	Shear	Parallel	Perpindicular to Bedding	23	5	Unable to discern	7319	Test stopped*
Limestone	3/8" Powers Wedge Bolt	Shear	Parallel	Perpindicular to Bedding	23	4	Unable to discern	7688	Test stopped*
Limestone	3/8" Powers Wedge Bolt	Shear	Parallel	Perpindicular to Bedding	23	3	Unable to discern	7470	Test stopped*
Limestone	3/8" Powers Wedge Bolt	Shear	Parallel	Perpindicular to Bedding	23	6	7900	9241	Test stopped*
Limestone	3/8" Powers Wedge Bolt	Shear	Parallel	Perpindicular to Bedding	16	3	Unable to discern	7540	Test stopped*
Limestone	3/8" Powers Power Stud	Shear	Parallel	Shear	11	1	4200	4511	Bolt sheared
Limestone	3/8" Powers Power Stud	Shear	Parallel	Shear	11	2	3500	4511	Bolt sheared
Limestone	3/8" Powers Power Stud	Shear	Parallel	Shear	21	2	3800	4511	Bolt sheared
Limestone	3/8" Powers Power Stud	Shear	Parallel	Shear	21	1	3700	4554	Bolt sheared
Limestone	3/8" Powers Power Stud	Shear	Parallel	Shear	20	2	3700	4308	Bolt sheared
Limestone	3/8" Powers Power Stud	Shear	Parallel	Shear	20	1	3900	4741	Bolt sheared
Limestone	3/8" Powers Power Stud	Shear	Parallel	Shear	18	1	3200	4475	Bolt sheared
Limestone	3/8" Powers Power Stud	Shear	Parallel	Shear	18	2	3300	4475	Bolt sheared
Limestone	3/8" Powers Wedge Bolt	Shear	Parallel	Shear	13	2	Unable to discern	7277	Test stopped*
Limestone	3/8" Powers Wedge Bolt	Shear	Parallel	Shear	13	1	Unable to discern	7218	Test stopped*
Limestone	3/8" Powers Wedge Bolt	Shear	Parallel	Shear	23	1	Unable to discern	7243	Test stopped*
Limestone	3/8" Powers Wedge Bolt	Shear	Parallel	Shear	23	2	Unable to discern	7428	Test stopped*
Limestone	3/8" Powers Wedge Bolt	Shear	Parallel	Shear	16	1	Unable to discern	7310	Test stopped*
Limestone	3/8" Powers Wedge Bolt	Shear	Parallel	Shear	16	2	Unable to discern	7419	Test stopped*
Limestone	3/8" Powers Wedge Bolt	Shear	Parallel	Shear	22	2	Unable to discern	7679	Test stopped*
Limestone	3/8" Powers Wedge Bolt	Shear	Parallel	Shear	22	1	7500	9035	Test stopped*
Sandstone	3/8" Powers Power Stud	Shear	Parallel	Parallel to Bedding	9	4	Unable to discern	3595	Bolt sheared
Sandstone	3/8" Powers Power Stud	Shear	Parallel	Parallel to Bedding	9	6	3000	3763	Bolt sheared
Sandstone	3/8" Powers Power Stud	Shear	Parallel	Parallel to Bedding	20	4	2900	4058	Bolt sheared
Sandstone	3/8" Powers Power Stud	Shear	Parallel	Parallel to Bedding	20	5	2800	3679	Bolt sheared
Sandstone	3/8" Powers Power Stud	Shear	Parallel	Parallel to Bedding	20	3	3200	3670	Bolt sheared
Sandstone	3/8" Powers Power Stud	Shear	Parallel	Parallel to Bedding	20	6	2400	3814	Bolt sheared
Sandstone	3/8" Powers Power Stud	Shear	Parallel	Parallel to Bedding	10	4	3200	3907	Bolt sheared
Sandstone	3/8" Powers Power Stud	Shear	Parallel	Parallel to Bedding	10	3	2800	4252	Bolt sheared
Sandstone	3/8" Powers Power Stud	Shear	Parallel	Parallel to Bedding	10	5	3200	4101	Bolt sheared
Sandstone	3/8" Powers Power Stud	Shear	Parallel	Parallel to Bedding	10	6	3200	3822	Bolt sheared
Sandstone	3/8" Powers Wedge Bolt	Shear	Parallel	Parallel to Bedding	14	3	Unable to discern	8960	Test stopped*
Sandstone	3/8" Powers Wedge Bolt	Shear	Parallel	Parallel to Bedding	14	4	Unable to discern	8192	Cube split in half
Sandstone	3/8" Powers Wedge Bolt	Shear	Parallel	Parallel to Bedding	38	4	Unable to discern	7612	Test stopped*
Sandstone	3/8" Powers Wedge Bolt	Shear	Parallel	Parallel to Bedding	35	5	6800	7270	Cube split in half
Sandstone	3/8" Powers Wedge Bolt	Shear	Parallel	Parallel to Bedding	38	6	Unable to discern	5611	Cube split in half
Sandstone	3/8" Powers Wedge Bolt	Shear	Parallel	Parallel to Bedding	13	4	6700	7729	Cube split in half
Sandstone	3/8" Powers Wedge Bolt	Shear	Parallel	Parallel to Bedding	32	4	6400	6831	Cube split in half
Sandstone	3/8" Powers Wedge Bolt	Shear	Parallel	Parallel to Bedding	18	3	Unable to discern	8081	Cube split in half
Sandstone	3/8" Powers Wedge Bolt	Shear	Parallel	Parallel to Bedding	11	5	Unable to discern	6179	Cube split in half
Sandstone	3/8" Powers Power Stud	Shear	Parallel	Perpindicular to Bedding	15	5	2900	3053	Bolt sheared
Sandstone	3/8" Powers Power Stud	Shear	Parallel	Perpindicular to Bedding	15	6	2500	3760	Bolt sheared
Sandstone	3/8" Powers Power Stud	Shear	Parallel	Perpindicular to Bedding	15	4	2800	3206	Bolt sheared
Sandstone	3/8" Powers Power Stud	Shear	Parallel	Perpindicular to Bedding	15	3	Unable to discern	3380	Bolt sheared
Sandstone	3/8" Powers Power Stud	Shear	Parallel	Perpindicular to Bedding	12	6	Unable to discern	3121	Bolt sheared
Sandstone	3/8" Powers Power Stud	Shear	Parallel	Perpindicular to Bedding	15	2	2600	3062	Bolt sheared
Sandstone	3/8" Powers Power Stud	Shear	Parallel	Perpindicular to Bedding	12	4	Unable to discern	3611	Bolt sheared
Sandstone	3/8" Powers Power Stud	Shear	Parallel	Perpindicular to Bedding	12	3	Unable to discern	3746	Bolt sheared
Sandstone	3/8" Powers Power Stud	Shear	Parallel	Perpindicular to Bedding	9	3	3200	3645	Bolt sheared
Sandstone	3/8" Powers Power Stud	Shear	Parallel	Perpindicular to Bedding	9	5	3100	3982	Bolt sheared
Sandstone	3/8" Powers Wedge Bolt	Shear	Parallel	Perpindicular to Bedding	31	6	Unable to discern	7637	Bolt sheared
Sandstone	3/8" Powers Wedge Bolt	Shear	Parallel	Perpindicular to Bedding	31	5	7300	8281	Bolt sheared
Sandstone	3/8" Powers Wedge Bolt	Shear	Parallel	Perpindicular to Bedding	21	4	7500	8213	Bolt sheared
Sandstone	3/8" Powers Wedge Bolt	Shear	Parallel	Perpindicular to Bedding	31	4	Unable to discern	9502	Test stopped*
Sandstone	3/8" Powers Wedge Bolt	Shear	Parallel	Perpindicular to Bedding	21	6	Unable to discern	7767	Bolt sheared
Sandstone	3/8" Powers Wedge Bolt	Shear	Parallel	Perpindicular to Bedding	31	3	8100	9342	Instron Overloaded
Sandstone	3/8" Powers Wedge Bolt	Shear	Parallel	Perpindicular to Bedding	21	5	Unable to discern	6967	Cube split in half
Sandstone	3/8" Powers Wedge Bolt	Shear	Parallel	Perpindicular to Bedding	16	4	Unable to discern	9191	Instron Overloaded
Sandstone	3/8" Powers Wedge Bolt	Shear	Parallel	Perpindicular to Bedding	32	5	7200	8983	Test stopped*
Sandstone	3/8" Powers Wedge Bolt	Shear	Parallel	Perpindicular to Bedding	18	5	8300	9300	Test stopped*
Sandstone	3/8" Powers Power Stud	Shear	Parallel	Shear	12	2	3200	3884	Bolt sheared
Sandstone	3/8" Powers Power Stud	Shear	Parallel	Shear	12	1	3400	4303	Bolt sheared
Sandstone	3/8" Powers Power Stud	Shear	Parallel	Shear	9	1	3200	4210	Bolt sheared

APPENDIX B: SHEAR RESULTS (continued)

Sandstone	3/8" Powers Power Stud	Shear	Parallel	Shear	9	2	3200	4370	Bolt sheared
Sandstone	3/8" Powers Power Stud	Shear	Parallel	Shear	10	2	Unable to discern	4060	Bolt sheared
Sandstone	3/8" Powers Power Stud	Shear	Parallel	Shear	10	1	Unable to discern	4379	Bolt sheared
Sandstone	3/8" Powers Power Stud	Shear	Parallel	Shear	15	1	3200	4117	Bolt sheared
Sandstone	3/8" Powers Power Stud	Shear	Parallel	Shear	15	2	Unable to discern	4573	Bolt sheared
Sandstone	3/8" Powers Power Stud	Shear	Parallel	Shear	20	1	3400	4354	Bolt sheared
Sandstone	3/8" Powers Power Stud	Shear	Parallel	Shear	20	2	4000	4320	Bolt sheared
Sandstone	3/8" Powers Wedge Bolt	Shear	Parallel	Shear	21	1	Unable to discern	7354	Test stopped*
Sandstone	3/8" Powers Wedge Bolt	Shear	Parallel	Shear	35	1	Unable to discern	7313	Test stopped*
Sandstone	3/8" Powers Wedge Bolt	Shear	Parallel	Shear	21	2	Unable to discern	7429	Test stopped*
Sandstone	3/8" Powers Wedge Bolt	Shear	Parallel	Shear	35	2	Unable to discern	8680	Test stopped*
Sandstone	3/8" Powers Wedge Bolt	Shear	Parallel	Shear	36	2	Unable to discern	6283	Slipped out
Sandstone	3/8" Powers Wedge Bolt	Shear	Parallel	Shear	23	2	Unable to discern	8847	Test stopped*
Sandstone	3/8" Powers Wedge Bolt	Shear	Parallel	Shear	23	1	Unable to discern	6189	Face delamination
Sandstone	3/8" Powers Wedge Bolt	Shear	Parallel	Shear	11	1	Unable to discern	7620	Test stopped*
Sandstone	3/8" Powers Wedge Bolt	Shear	Parallel	Shear	11	2	Unable to discern	7901	Face delamination
Sandstone	3/8" Powers Wedge Bolt	Shear	Parallel	Shear	36	1	Unable to discern	6845	Bolt sheared

APPENDIX C: LOAD CELL CALIBRATION

To calibrate the Instron's 10,000-pound tensile load cell (serial 508F), Vertical Access uses a Dillon 10,000-pound analog dynamometer (serial D32843), accurate to +/- 0.5% of capacity. The following information describes the calibration process, which was conducted every day prior to testing

The dynamometer is first zeroed using the zero control knob on the back of the unit.

The dynamometer hangs from the load cell and is connected to the cross head with a length of 2-inch nylon webbing. To calibrate the load cell, Vertical Access uses 13 data points spaced 500 lbf apart. The crosshead is moved down until the dynamometer reads approximately 500 lbf. As soon as the crosshead stops moving, the webbing will begin to creep and the tension will decrease. The maximum force, as indicated by the red pointer, is recorded. The second photo shows that the dynamometer was loaded to approximately 3000 lbf then the webbing crept and the tension slowly dropped to 2200 lbf. A force of 3050 lbf was recorded for this load.

Next, the dynamometer is loaded to approximately 1000 lbf and the actual load is recorded again. This process continues for 500 lbf increments up to 6000 lbf.

The voltage data from the load cell is recording using LabJack's LJStream software via a USB connection. Once the calibration voltage stream is recorded, the data is graphed to produce a chart similar to the one below.

Note in the following figure that the vertical axis represents voltage and each peak in the data corresponds to one of the loads recorded in 500 lbf increments. Using a table similar to the one below, a linear regression of the data can easily be performed. The "Load" column lists all of the values recorded from the dynamometer. Note that zero is included as the first data point. The "Voltage" column lists the peak voltages that correspond to each load.

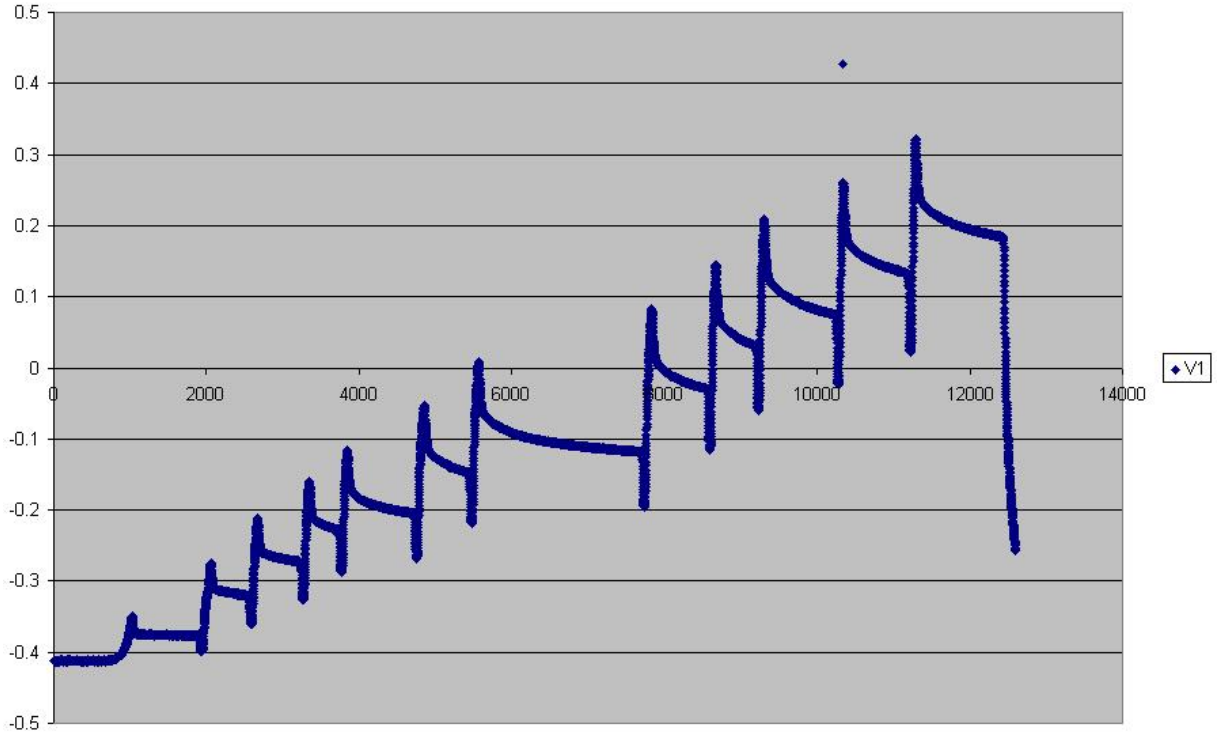

Voltage	Load
	0
	500
	1100
	1600
	2100
	2450
	3000
	3450
	4100
	4600
	5150
	5575
	6075
slope:	
intercept:	
int/slope:	

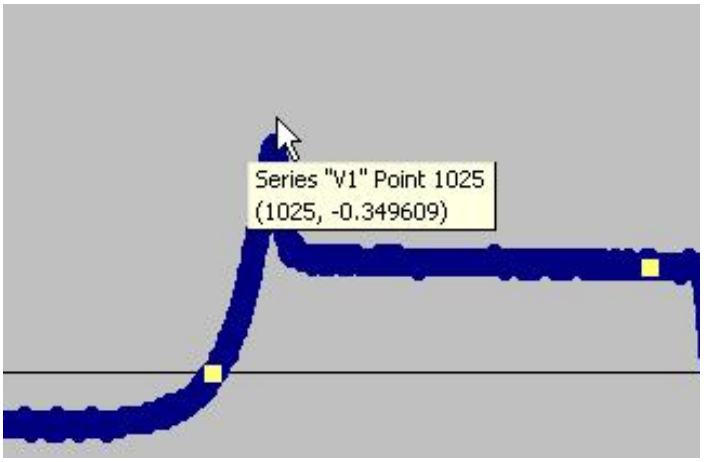

Voltage	Load
-0.41113	0
-0.34961	500
-0.27441	1100
-0.21289	1600
-0.16016	2100
-0.11719	2450
-0.05176	3000
0.007812	3450
0.080078	4100
0.144531	4600
0.208984	5150
0.259766	5575
0.322266	6075
slope:	8320.264
intercept:	3408.232
int/slope:	0.40963

Once all of the voltage cells are filled, Excel's linear regression tools are used to find the necessary scaling equation. In the slope cell, the "=slope(y,x)" function calculates the slope of the scaling equation. Similarly, the "=intercept(y,x)" function calculates the intercept of the scaling equation. Calculating the intercept to slope ratio will show the negative of the load cell's base voltage output.

The scaling equation defined by the data above can be written two ways:
Y = (8320.264 * v) + 3408.232
Y = (v + 0.40963) * 8320.264.

The equation is entered into the LabJack software, which will read the load cell's voltage and output the corresponding load (lbf).

The load cell's resistance is linearly proportional to its strain, which is why we are able to use a linear equation to convert voltage to load. Another property of the load cell is that its resistance is very stable over time, meaning that the scaling equation determined today should be very similar to the equation determined a year ago. Comparing the newly computed equation to previously used equations serves as a quick error check. The following graph shows the various calibration equations used while testing mechanical anchors in dimensioned stone.